Inorganic Chemistry

Article

pubs.acs.org/IC

Two Acentric Mononuclear Molecular Complexes with Unusual Magnetic and Ferroelectric Properties

Fang-Hua Zhao, Yun-Xia Che, and Ji-Min Zheng*

Department of Chemistry, Nankai University, Tianjin 300071, China

Fernande Grandjean and Gary J. Long*

Department of Chemistry, Missouri University of Science and Technology, University of Missouri, Rolla, Missouri 65409-0010, United States

Supporting Information

ABSTRACT: Two acentric, i.e., noncentrosymmetric, mononuclear complexes, Co(5-ATZ)$_4$Cl$_2$, **1**, and Cu(5-ATZ)$_4$Cl$_2$, **2**, where 5-ATZ is the monodentate 5-amino-1-H-tetrazole ligand, have been prepared and characterized. Both complexes crystallize in the tetragonal system with the *P*4*nc* space group, a member of the polar non-centrosymmetric 4*mm* class, and thus both **1** and **2** can exhibit ferroelectric and nonlinear optical properties. Magnetic studies indicate that **1** is a paramagnetic high-spin cobalt(II) complex with a rather extensive spin−orbit coupling, modeled as a zero-field splitting parameter, *D*, of ±91(3) cm^{-1} and with very weak long-range antiferromagnetic exchange interactions. Direct current (dc) and ac magnetic studies indicate that **2** is a paramagnetic copper(II) complex that exhibits weak ferromagnetic exchange interactions below 15 K. Both **1** and **2** exhibit ferroelectric hysteresis loops at room temperature with remanent polarizations of 0.015 μC/cm^2 and coercive electric fields of 5.5 and 5.7 kV/cm, respectively.

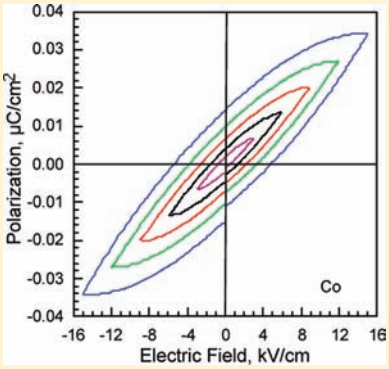

INTRODUCTION

Ferroelectric coordination complexes are of interest because of their promising applications in a variety of new technologies, such as electric devices, information storage, and nonlinear optical devices.[1] For a complex to exhibit ferroelectricity, the complex must crystallize in one of the 10 polar non-centrosymmetric crystal classes, namely, 1, *m*, 2, *mm*2, 3, 3*m*, 4, 4*mm*, 6, and 6*mm* crystal classes.[2−4]

Multifunctional materials are especially attractive for technological applications because their properties can be controlled through two external parameters, i.e., in the case of a multiferroic complex, an applied electric field and an applied magnetic field.

Fortunately, the 10 polar noncentrosymmetric crystal classes listed above offer the possibility of multifunctionality[3] as the 1, 2, 3, 4, and 6 crystal classes can exhibit a combination of chirality, enantiomorphism, optical activity, ferroelectricity, and piezoelectricity, whereas the *m* and *mm*2 crystal classes can exhibit optical activity, ferroelectricity, and piezoelectricity, and the 3*m*, 4*mm*, and 6*mm* crystal classes can exhibit only ferroelectricity and piezoelectricity. Further, if a complex contains transition metal ions with unpaired electrons, a combination of the resulting magnetic properties with the above properties may induce novel functions and may possibly lead, for instance, to a multiferroic complex exhibiting the coexistence of both ferromagnetic and ferroelectric properties.[5]

Although a great deal of progress has been made in the syntheses of ferroelectric complexes,[1c,2,6] challenges still remain in the systematic engineering[7] of crystalline complexes that exhibit polar order.

Because of the close relationship that exists between chirality and ferroelectricity in the 1, 2, 3, 4, and 6 crystal classes, one efficient synthetic strategy to prepare ferroelectric complexes is to use chiral organic ligands that form a homochiral structure,[2] i.e., a geometric arrangement in a crystal in which all the chiral ligands show the same dextrorotary or levorotary chirality. Another more challenging synthetic strategy[7,8] is to use achiral organic ligands. Such ligands may be included[8a] in chiral coordination polymers by spontaneous resolution, polymers that may also exhibit ferromagnetism. In other cases, an achiral organic ligand may induce[6a,6] chirality in the complex because of its flexibility or simply lead to a complex crystallizing in a noncentrosymmetric crystal class. Many of these complexes exhibit ferroelectric and/or nonlinear optical properties.

The 5-amino-1-H-tetrazole ligand, herein referred to as 5-ATZ, is a potentially multidentate ligand whose tetrazole ring nitrogens may bridge between transition metal ions in various coordination modes; a few recent examples of 5-ATZ coordination complexes have been reported.[9] However, these studies have mainly concentrated on either their novel

Received: February 21, 2012
Published: April 5, 2012

topological architectures or their photoluminescent properties and so far rarely concern the development of their magnetic and ferroelectric properties.

Herein, we report the syntheses, structures, and magnetic and ferroelectric properties of two polar noncentrosymmetric mononuclear coordination complexes, $Co(5\text{-}ATZ)_4Cl_2$, **1**, and $Cu(5\text{-}ATZ)_4Cl_2$, **2**, complexes that represent the first examples of polar noncentrosymmetric complexes based on the achiral 5-ATZ ligand.

EXPERIMENTAL SECTION

Chemical reagents and solvents were purchased commercially and used as received without further purification. The crystals of **1** and **2** are very stable in air at ambient temperature and are insoluble in water and common organic solvents.

Synthesis of $Co(5\text{-}ATZ)_4Cl_2$, 1. A mixture of $CoCl_2{\cdot}6H_2O$ (0.24 g, 1.0 mmol) and 5-ATZ (0.34 g, 4.0 mmol) was dissolved in 40 mL of distilled water by stirring for 4 h at 80 °C. Red block-shaped single crystals were obtained as the solvent slowly evaporated at ambient temperature over a period of 5 days. The yield was 75% based on Co. Elemental analysis calcd for $CoC_4H_{12}N_{20}Cl_2$: C, 10.22%, H, 2.57%, and N, 59.59%. Observed: C, 10.16%, H, 2.60%, and N, 59.63%. Infrared absorptions in cm^{-1} measured in KBr: 3444s, 3339s, 3225w, 1642s, 1577w, 1462w, 1396w, 1297m, 1135m, 1056m, 997m, 712w, 628w, and 444w.

Synthesis of $Cu(5\text{-}ATZ)_4Cl_2$, 2. A mixture of $CuCl_2{\cdot}2H_2O$ (0.17 g, 1.0 mmol) and 5-ATZ (0.34 g, 4.0 mmol) was dissolved in 40 mL of distilled water by stirring for 4 h at 80 °C. Blue block-shaped single crystals were obtained as the solvent slowly evaporated at ambient temperature over a period of 5 days. The yield was 64% based on Cu. Elemental analysis calcd for $CuC_4H_{12}N_{20}Cl_2$: C, 10.12%, H, 2.55%, and N, 59.01%. Observed: C, 10.10%, H, 2.60%, and N, 59.03%. Infrared absorptions in cm^{-1} measured in KBr: 3424s, 3332s, 3141w, 1641s, 1578w, 1466m, 1300m, 1141m, 1059m, 1000m, 726w, and 461w.

Physical Methods. Elemental analyses were performed by using a Perkin-Elmer Model 240 CHN elemental analyzer. Infrared spectra were obtained between 4000 and 400 cm^{-1} in KBr pellets by using a Nicolet Magna-IR 560 infrared spectrometer.

Electric Studies. Electric hysteresis loops have been measured at ambient temperature by using a Premier II ferroelectric instrument. The ambient temperature electric polarization of 0.1 cm thick pressed pellets made from polycrystalline samples of **1** and **2** was measured at ±300, ±600, ±900, ±1200, and ±1500 V or in applied fields of ±3, ± 6, ± 9, ± 12, and ±15 kV/cm. The accuracy on the measured electric polarization is 0.001 $\mu C/cm^2$.

Magnetic Studies. Magnetic studies were performed on samples of **1** and **2** anchored in eicosane by using either a Quantum Design MPMS superconducting quantum interference magnetometer or a Maglab 2000 magnetometer. The dc magnetic susceptibility of **1** was measured during field cooling from 270 to 2 K in a 0.1 T applied field. The dc magnetic susceptibility of **2** was measured during field cooling from 300 to 2 K followed by field warming to 300 K in a 0.1 T applied field; between 15 and 300 K the cooling and warming results were essentially identical and have been merged. The dc magnetization of **2** was subsequently measured at 2 K between ±4 T. Subsequently, the ac magnetization of **2** was measured in a ± 3 Oe ac field at seven frequencies between 311 and 2311 Hz during warming from 2 to 30 K in a zero dc bias field. Next, the ac magnetization of **2** was measured in a ± 3 Oe ac field at 11 frequencies between 111 and 9011 Hz during warming from 2 to 30 K in the presence of a 0.1 T dc bias field. Finally, the ac magnetization of **2** was measured in a ±3 Oe ac field at 14 frequencies between 311 and 9011 Hz during warming from 2 to 20 K in the presence of a 0.2 T dc bias field. Diamagnetic corrections of −0.000 214 and −0.000 215 emu/mol, obtained from tables of Pascal's constants,[10] have been applied to all the measured molar magnetic susceptibilities of **1** and **2**, respectively. The errors associated with the various magnetic fits reported below are the statistical fitting errors; the actual errors are probably 2−3 times larger.

X-ray Crystallographic Studies. Suitable single crystals of **1** and **2** were selected and mounted in air on thin glass fibers. Accurate unit cell parameters were determined by a least-squares fit of 2θ values, and the intensity data were measured at 153(2) K for **1** and 294(2) K for **2** by using a Rigaku R-axis Rapid IP area detector with 0.710 73 Å Mo K_α radiation. The intensities were corrected for Lorentz and polarization effects as well as for empirical absorption by using the multiscan technique.[11] All structures were solved by direct methods and refined by full-matrix least-squares fitting on F^2 by using the SHELX-97 code.[12] All non-hydrogen atoms were refined with anisotropic thermal parameters. The positions of the hydrogen atoms bound to the nitrogen of a tetrazole ring and to the amino group were calculated theoretically. The refined Flack parameter[13] is 0.036(15) for **1** and 0.023(15) for **2**, values that indicate that the absolute structures are well-defined.

RESULTS AND DISCUSSION

Single Crystal Structural Results. Single-crystal X-ray structural studies indicate that **1** and **2** are isostructural and crystallize in the tetragonal system with the *P*4*nc* space group, a member of the polar noncentrosymmetric 4*mm* class, and thus both $Co(5\text{-}ATZ)_4Cl_2$, **1**, and $Cu(5\text{-}ATZ)_4Cl_2$, **2**, can exhibit pyroelectric and ferroelectric properties as well as second harmonic generation nonlinear optical properties.[3,9] The unit cells of **1** and **2** have $Z = 2$ and thus there are two molecules of the complex per unit cell, one of which resides near the center of the unit cell and the second lies on four *c*-edges of the unit cell. Although an isolated molecule of **1** and **2** would be chiral, see Figure 1, in the crystalline solid state both **1** and **2** are

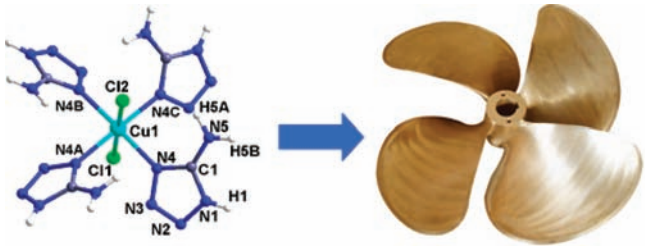

Figure 1. The X-ray structure of $Cu(5\text{-}ATZ)_4Cl_2$, **2**, obtained at 294(2) K, left, and its chirality as an isolated molecule, right.

achiral because of the symmetry operations associated with the space group that generate the two symmetry related molecules found in the unit cells.

Details of the crystal and structural refinement are given in ref 14, and selected bond distances and angles are given in Table 1.

Complexes **1** and **2** are isostructural and both are self-assembled from the achiral 5-amino-1-H-tetrazole, 5-ATZ, ligand. Because of the close similarity of the two structures, only the structure of **2** will be described in detail. The asymmetric unit of **2** consists of one copper(II) cation, two chloride anions, and one 5-ATZ ligand. The molecular structure of **2** is shown in Figure 1 and that of **1** is shown in Figure S1 in the Supporting Information.

The copper(II) ion in **2** is six-coordinate with four coordinated nitrogen atoms from four 5-ATZ ligands forming the equatorial plane and two trans chloride anions in the axial positions to yield the *trans*-CuN_4Cl_2 pseudo-octahedral structure. The copper(II) ion exhibits a "classic" Jahn−Teller distortion, with two significantly different copper(II) to

dx.doi.org/10.1021/ic300394c | Inorg. Chem. 2012, 51, 4862−4868

Table 1. Selected Bond Lengths (Å) and Bond Angles (deg) for 1 and 2[a]

		complex 1			
Co(1)−Cl(1)	2.4332(10)	N(4)no.1−Co(1)−N(4)no.2	89.956(3)	N(4)no.2−Co(1)−Cl(1)	91.59(5)
Co(1)−Cl(2)	2.5411(10)	N(4)−Co(1)−N(4)no.2	89.956(3)	N(4)no.3−Co(1)−Cl(1)	91.59(5)
Co(1)−N(4)	2.1265(11)	N(4)no.1−Co(1)−N(4)no.3	89.956(3)	N(4)no.1−Co(1)−Cl(2)	88.41(5)
Co(1)−N(4) no.1	2.1265(11)	N(4)−Co(1)−N(4)no.3	89.956(3)	N(4)−Co(1)−Cl(2)	88.41(5)
Co(1)−N(4)no.2	2.1265(11)	N(4)no.2−Co(1)−N(4)no.3	176.82(10)	N(4)no.2−Co(1)−Cl(2)	88.41(5)
Co(1)−N(4)no.3	2.1265(12)	N(4)no.1−Co(1)−Cl(1)	91.59(5)	N(4)no.3−Co(1)−Cl(2)	88.41(5)
N(4)no.1−Co(1)−N(4)	176.82(10)	N(4)−Co(1)−Cl(1)	91.59(5)	Cl(1)−Co(1)−Cl(2)	180.0
		complex 2			
Cu(1)−N(4)	2.0217(15)	N(4)−Cu(1)−N(4)no.2	175.40(13)	N(4)no.2−Cu(1)−Cl(2)	92.30(7)
Cu(1)−N(4)no.1	2.0217(15)	N(4)no.1−Cu(1)−N(4)no.2	89.908(5)	N(4)no.3−Cu(1)−Cl(2)	92.30(7)
Cu(1)−N(4)no.2	2.0217(15)	N(4)−Cu(1)−N(4)no.3	89.908(5)	N(4)−Cu(1)−Cl(1)	87.70(7)
Cu(1)−N(4)no.3	2.0217(15)	N(4)no.1−Cu(1)−N(4)no.3	175.40(13)	N(4)no.1−Cu(1)−Cl(1)	87.70(7)
Cu(1)−Cl(1)	2.8099(12)	N(4)no.2−Cu(1)−N(4)no.3	89.908(5)	N(4)no.2-Cu(1)−Cl(1)	87.70(7)
Cu(1)−Cl(2)	2.6076(13)	N(4)−Cu(1)−Cl(2)	92.30(7)	N(4)no.3−Cu(1)−Cl(1)	87.70(7)
N(4)−Cu(1)−N(4)no.1	89.908(5)	N(4)no.1−Cu(1)−Cl(2)	92.30(7)	Cl(2)−Cu(1)−Cl(1)	180.0

[a]Symmetry operations: for **1**, no.1 $-y, x, z$; no.2 $-x, -y, z$; no.3 $y, -x, z$. For **2**, no.1 $-x + 2, -y + 2, z$; no.2 $y, -x + 2, z$; no.3 $-y + 2, x, z$.

chloride trans bond distances of 2.8099(12) Å for the Cu−Cl1 bond and 2.6076(13) Å for the Cu−Cl2 bond; the four equatorial Cu−N4 bond distances are significantly shorter at 2.0217(15) Å. The copper(II) ion is 0.0815 Å above the center of the plane of the four equatorial coordinated N4 nitrogens in the direction of Cl2. Further, Cl1 is 2.7284 Å and Cl2 is 2.6891 Å from the center of the plane formed by the four equatorial N4 coordinated nitrogens. However, it should be noted that the four N5 atoms of the four 5-amino groups on the 5-ATZ ligands are all above the plane of the N4 atoms and thus are all found in the direction of Cl2; the distance of Cl2 to the four H5A hydrogens of these amino groups is 2.848 Å. Because of steric crowding one might expect the Cu−Cl2 distance to be longer than the Cu−Cl1. However, this is *not* the case and it seems that Cl2 is pulled closer to the copper(II) ion than is Cl1 by weak bonding interactions of Cl2 with the H5A hydrogen of the 5-amino group on the four 5-ATZ ligands.

A very similar bonding situation occurs in $Co(5\text{-}ATZ)_4Cl_2$, **1**, although the actual bond distances are rather different, i.e., the cobalt(II) ion is only 0.0586 Å above the center of the plane of the four equatorial coordinated N4 nitrogens and the Co−Cl1 and Co−Cl2 bond distances are 2.541 and 2.433 Å, respectively. At this point, the reader must note that numbering of the chloride ions is inverted in the two structures, see Figure 1 and Figure S1 in the Supporting Information.

The tetrazole rings of the four 5-ATZ ligands in **1** and **2** are not coplanar but rather they are arranged like the blades of a propeller, see Figure 1, with an adjacent dihedral angle of 59.79°; the trans tetrazole-rings are almost perpendicular to each other with a dihedral angle of 89.67°.

In **1** and **2** the eight shortest intermolecular Co−Co and Cu−Cu bond distances are 8.070(8) and 8.0521(8) Å, respectively; there are no significant intermolecular contact interactions between the molecules. In **2** the shortest hydrogen bonds are the N5−H5A···N2 bond of 3.339(3) Å and the N5−H5B···N3 bond of 3.277(3) Å; in this case, these weak intermolecular hydrogen bonds may be negligible but could possibly lead to long-range magnetic exchange at very low temperatures.

Magnetic Properties of $Co(5\text{-}ATZ)_4Cl_2$, 1. The temperature dependence of $\chi_M T$ of **1**, which has been measured upon cooling from 270 to 2 K in a 0.1 T applied field, indicates both that $\chi_M T$ decreases continually between 270 and 2 K and that $1/\chi_M$ is virtually linear between 50 and 270 K. The temperature dependence of $1/\chi_M$, see the inset to Figure 2, has been fit between 50 and 270 K with the Curie−Weiss law and yields a Weiss temperature, θ, of −38(1) K, a Curie constant, C, of 3.47(1) emu K/mol, a corresponding effective magnetic moment, μ_{eff}, of 5.268(4) μ_B and, for $S = {}^3/_2$, a g-factor of 2.720(2).

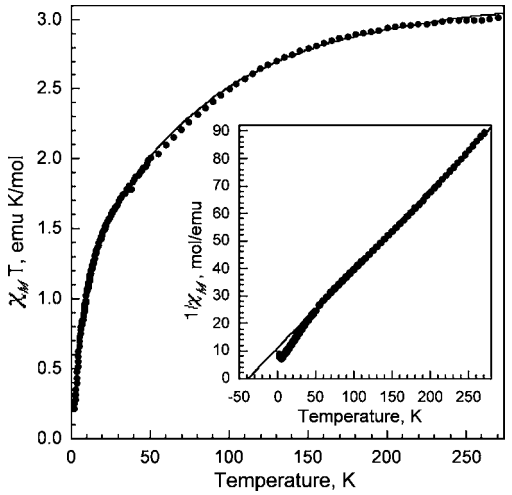

Figure 2. Temperature dependence of $\chi_M T$ of $Co(5\text{-}ATZ)_4Cl_2$, **1**, obtained upon cooling from 270 to 2 K in a 0.1 T applied field and fit for $S = {}^3/_2$ with $g = 2.655(6)$, $D = 91(3)$ cm^{-1}, and $zJ = -0.614(6)$ cm^{-1}. Inset: the inverse molar magnetic susceptibility, $1/\chi_M$, of **1** with a 50−270 K Curie−Weiss law fit.

The 270 to 2 K temperature dependence of $\chi_M T$ for **1** has been fit[17,18] by including the influence of spin−orbit coupling on the cobalt(II) ion ground state, an influence that is treated as a zero-field splitting for an $S = {}^3/_2$ cobalt(II) ion in the presence of the approximately axially distorted octahedral coordination environment found in **1**. Preliminary fits with this approach indicated that the $\chi_M T$ observed at lower temperatures was lower than is possible with this model. Indeed, the lower values indicate the presence of weak long-range antiferromagnetic order that becomes most important at low temperatures. Thus the $\chi_M T$ for **1** has been fit with the expression

dx.doi.org/10.1021/ic300394c | Inorg. Chem. 2012, 51, 4862−4868

$$\chi_M T = \frac{\chi_M' T}{1 - (2zJ/Ng^2\mu_B^2)\chi_M'}$$

where χ_M' is the molar susceptibility in the presence of the zero-field splitting mentioned above and zJ approximates the contribution of the molecular exchange field. The result of this fit is shown by the solid curve in Figure 2, where the best fit with $S = {}^3/_2$ yields a zero-field splitting, D, of $\pm 91(3)$ cm^{-1}, a g-value of 2.655(6), and $zJ = -0.614(6)$ cm^{-1}. In this approach, the cobalt(II) orbital moment has been incorporated in part into the large but reasonable[17,18] value of $D = \pm 91(3)$ cm^{-1}. In the absence of the magnetization curve obtained at 2 K, it is not possible to determine the sign of D.

An alternative fit discussed in detail by Lloret et al.[19] that would apply only to a strictly octahedral coordination environment is shown in Figure S2 in the Supporting Information. This somewhat poorer fit of $\chi_M T$ for **1**, which directly incorporates the cobalt(II) spin−orbit coupling, λ, and an orbital reduction factor, α, with $S = {}^3/_2$ and $g = 2$, yields $\alpha = 1.30(1)$, $\lambda = -120(3)$ cm^{-1} and $zJ = -0.49(1)$ cm^{-1}. The rather small but obvious misfit observed between 50 and 150 K may be due to the axial distortion of the pseudooctahedral coordination environment found in **1**.

The results of these fits indicate that **1** is basically a paramagnetic high-spin cobalt(II) complex with a rather extensive spin−orbit coupling, coupling that may be modeled[17,18] as extensive zero-field splitting, and very weak long-range antiferromagnetic exchange interactions at low temperatures with $zJ = -0.614(6)$ cm^{-1}. The closest intermolecular cobalt(II)−cobalt(II) distance of 8.070(2) Å is found between the two cobalt(II) ions in a unit cell. Although each chloride ion is hydrogen bonded to a neighboring tetrazole ring, it seems that the most likely long-range exchange pathway involves overlap between two tetrazole rings on adjacent molecules, rings that are separated by ∼4 Å. Thus a given cobalt(II) ion is exchange coupled through its four tetrazole ligands to four adjacent cobalt(II) ions with $z = 4$ and an average $J = -0.153(2)$ cm^{-1}. This rather small J-value seems to be consistent with such an exchange pathway but other pathways are surely possible.

Magnetic Properties of Cu(5-ATZ)$_4$Cl$_2$, 2. The temperature dependence of $\chi_M T$ of **2** has been measured upon cooling from 300 to 2 K in a 0.1 T applied field, see Figure 3; a subsequent warming from 2 to 300 K revealed a small thermal hysteresis between 2 and 15 K. Between 15 and 300 K the cooling and warming results were, as expected, virtually identical and have been merged. Upon cooling and subsequent warming from 300 to 15 to 300 K, $\chi_M T$ increases gradually from 0.420(1) emu K/mol at 300 K to 0.456(2) emu K/mol at 15 K; the corresponding μ_{eff} values are 1.833(5) μ_B at 300 K and 1.910(5) μ_B at 15 K.

The temperature dependence of $1/\chi_M$ of **2** is linear between 100 and 300 K, and a fit with the Curie−Weiss law, see the right inset to Figure 3, yields a Weiss temperature, θ, of 12.1(3) K, a Curie constant, C, of 0.4063(6) emu K/mol, a corresponding μ_{eff} of 1.803(2) μ_B and, for $S = {}^1/_2$, a g-factor of 2.082(2), values that are reasonable for a copper(II) ion in a pseudooctahedral coordination environment.

Upon cooling from 15 to 2 K, the $\chi_M T$ of **2** clearly reveals a small increase followed by a decrease upon subsequent warming from 2 to 15 K and an associated small but obvious hysteresis, see the left inset to Figure 3. At first one might assign these changes to a trace of ferromagnetic impurity, but this seems unlikely for several reasons. The most obvious impurity would be a trace of copper(II) chloride, which is not ferromagnetic but rather is antiferromagnetic below ∼5 K.[20]

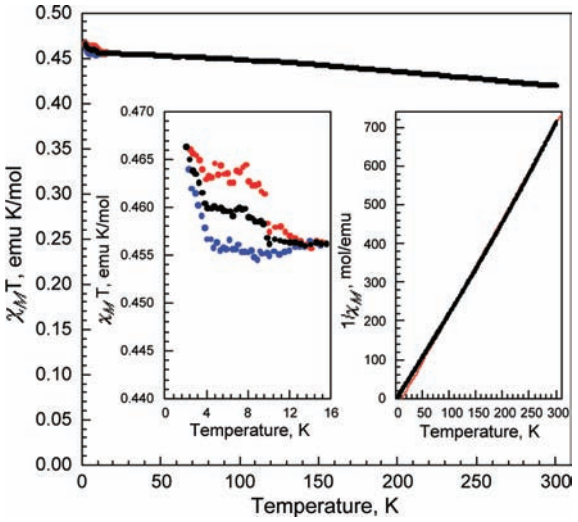

Figure 3. Temperature dependence of $\chi_M T$ of Cu(5-ATZ)$_4$Cl$_2$, **2**, obtained upon cooling from 300 to 2 K and subsequent warming to 300 K in a 0.1 T applied field. Left inset: the $\chi_M T$ of **2** obtained upon cooling from 15 to 2 K, blue, and subsequent warming to 15 K, red. The black points are the average of the cooling and warming results. Right inset: the inverse molar magnetic susceptibility, $1/\chi_M$, of **2** with a 100−300 K Curie−Weiss law fit shown in red.

As a consequence of the observed increase in $\chi_M T$ below 15 K, the 2 K magnetization and the ac susceptibility of **2** have been measured, and the results, see below, are rather inconsistent with the presence of any ferromagnetic impurity.

The molar magnetization of **2** has been measured at 2 K in an applied field of ±4 T; there is no detectable coercive field and hence no detectable hysteresis in the magnetization loops, see Figure S3 in the Supporting Information. Further, there is no detectable indication of any soft or hard ferromagnetic impurity present in **2**.

As is shown in Figure 4, a fit of the molar magnetization of **2** obtained in a separate measurement between 0 and 5 T at 2 K with a Brillouin function and $S = {}^1/_2$ and $g = 2.294(2)$ is excellent as would be expected for a paramagnetic copper(II) complex. Further, a linear fit of the 2 K molar magnetization of **2** between 0 and 10 000 Oe, see the inset to Figure 4, yields $\chi_M = 0.234(2)$ emu/mol and $\chi_M T = 0.468(4)$ emu K/mol at 2 K, a corresponding $\mu_{eff} = 1.94(1)$ μ_B and, for $S = {}^1/_2$, a g-factor of 2.23(1). All of these results are in excellent agreement with the results obtained at 2 K for **2** in a 0.1 T applied field, see above and Figure 3.

The molar magnetic susceptibility of **2** has been measured at several frequencies first upon warming from 2 to 30 K in a ±3 Oe ac field in a zero Oe bias field and then in a 1000 Oe dc bias field and, subsequently, upon warming from 2 to 20 K in a 2000 Oe dc bias field.

In the presence of a zero Oe bias field and a ±3 Oe ac field, the observed χ_M' molar magnetic susceptibility of **2** is independent of frequency between 311 and 2311 Hz and, as expected for a paramagnetic complex that relaxes rapidly on the measurement time scale of ∼0.5 ms, χ_M'' is always zero within experimental error. Thus, the top of Figure 5 shows only the susceptibilities obtained at 311 and 2311 Hz; the values at the remaining frequencies are virtually identical. A plot of $1/\chi_M'$ for

dx.doi.org/10.1021/ic300394c | Inorg. Chem. 2012, 51, 4862−4868

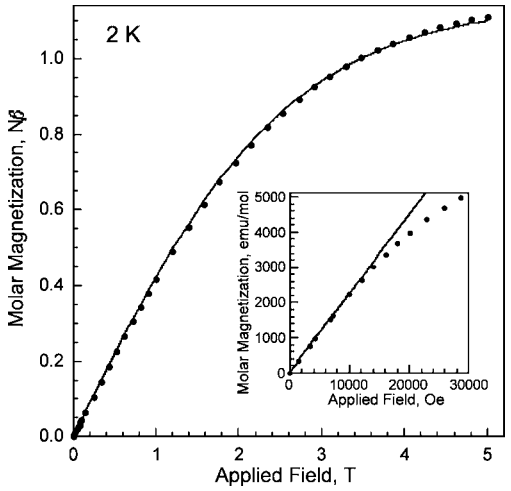

Figure 4. The field dependence of the molar magnetization of Cu(5-ATZ)$_4$Cl$_2$, **2**, obtained at 2 K with a fit, solid curve, with a Brillouin function with $S = {}^1/_2$ and $g = 2.294(2)$. Inset: the molar magnetization of **2** and a linear fit between 0 and 10 000 Oe, the slope of which at 2 K yields $\chi_M = 0.234(2)$ emu/mol and $\chi_M T = 0.468(4)$ emu K/mol.

the seven frequencies is linear from 2 to 30 K and yields a Curie constant, C, of 0.442(2) emu K/mol and $\theta = -0.1(5)$ K, where the ±0.002 emu K/mol and 0.5 K errors are the standard deviation in C and θ for the seven frequencies with a C that ranges from 0.439 to 0.444 emu K/mol; the corresponding $\mu_{eff} = 1.880(6)\ \mu_B$ and, for $S = {}^1/_2$, $g = 2.17(1)$. These values agree well with those obtained from the dc magnetic susceptibility measurements, see above.

As might be expected from the increase in $\chi_M T$ observed below 15 K for complex **2**, see the left inset to Figure 3, the $\chi_M' T$ obtained in a zero Oe bias field also shows a small increase in magnitude of the slope obtained between 2 and 15 K as compared to that observed between 15 and 30 K; this increase is present at all the seven frequencies studied, an increase in magnitude that is presumably associated with the onset or near onset of long-range weak ferromagnetic exchange coupling.

In contrast to the results obtained in the absence of a bias field, in the presence of a 1000 and 2000 Oe bias field, χ_M'' is not negligible, see the two lower portions of Figure 5. In the presence of the bias field, energy must be provided to the complex to facilitate its relaxation especially in the presence of the onset of weak ferromagnetic coupling. This transfer of energy is evidenced by the peak that develops in the temperature dependence of χ_M'', see Figure 5. The frequency dependence of this relaxation is most easily seen in the temperature dependence of $\chi_M'' T$ observed in the presence of a 1000 Oe bias field, see Figure 6, and in the presence of a 2000 Oe bias field, see Figure S4 in the Supporting Information. At 311 Hz and a 1000 Oe bias field, both $\chi_M' T$ and $\chi_M'' T$ are constant and the latter is essentially zero between 15 and 30 K. However, below 15 K, $\chi_M'' T$ increases slightly even as the temperature decreases and $\chi_M' T$ decreases substantially. In the presence of the bias fields, as the ±3 Oe ac field frequency increases from 311 to 2311 and 9011 Hz, the temperature of the peak in χ_M'' increases, see Figure 5. Further, as the bias field increases from 1000 to 2000 Oe, the temperature of the peak in χ_M'' also increases, see Figure 5. Such behavior suggests a decrease in the rate of magnetic relaxation in **2**.

Ferroelectric Properties. As is shown in Figure 7, both Co(5-ATZ)$_4$Cl$_2$, **1**, and Cu(5-ATZ)$_4$Cl$_2$, **2**, exhibit ferroelectric

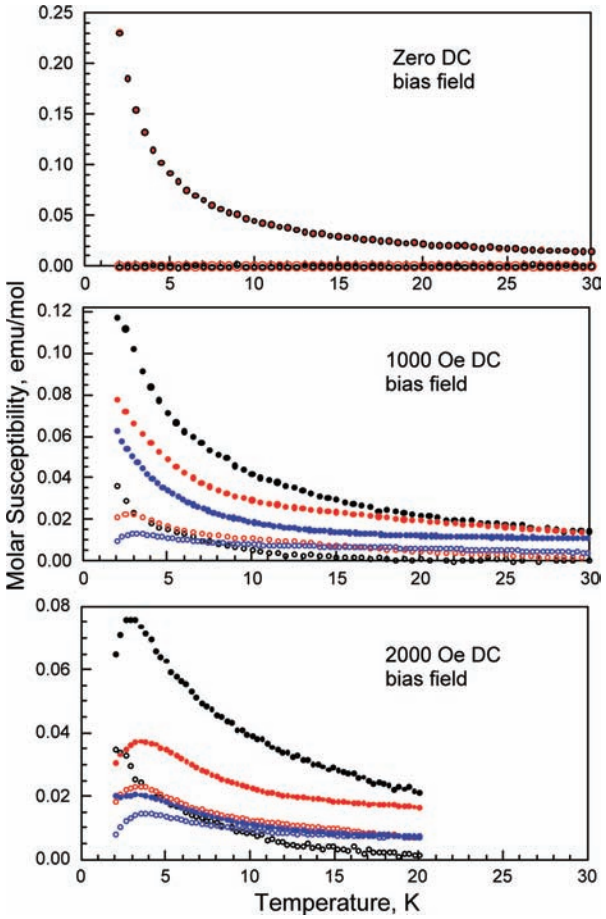

Figure 5. Temperature dependence of the ac molar magnetic susceptibilities, χ_M', solid points, and χ_M'', open points, for Cu(5-ATZ)$_4$Cl$_2$, **2**, obtained upon warming from 2 to 30 or 20 K in a ±3 Oe ac field and a 0, 1000, or 2000 Oe dc bias field. The black points have been obtained at 311 Hz, the red points at 2311 Hz, and the blue points at 9011 Hz. In the upper portion of the figure showing the results obtained in a zero dc field, the 311, 2311, and 9011 Hz data points all virtually overlap and only the 311 and 2311 Hz data are shown.

behavior presented here as electric hysteresis loops with remanent polarizations, P_r, of 0.015 μC/cm^2 for **1** and **2** and coercive fields, E_c, of 5.5 kV/cm for **1** and 5.7 kV/cm for **2**. The saturation of the spontaneous polarizations, P_s, of **1** and **2** are 0.034 and 0.031 μC/cm^2, respectively, both of which are smaller than the 0.25 μC/cm^2 observed[21] for Rochelle salt, $NaKC_4H_4O_6 \cdot 4H_2O$, a typical ferroelectric compound. The ferroelectric properties of **1** and **2** most likely result from the off-centering[1c] of the metal cation between the two axial chloride ligands, an off-centering that creates a spontaneous electric dipole moment. However, a simple electrostatic model, which assumes one negative elementary point charge on each chlorine and two positive elementary point charges on the metal cation at the positions determined from the X-ray diffraction patterns at 153 and 294 K, leads to an expected saturation polarization of 0.8 and 0.4 μC/cm^2 for perfect single crystal samples of **1** and **2**, respectively. The observed saturation polarizations are much smaller partly because they are measured on pressed pellets, whose volumes differ from the volume of crystalline samples. The small observed polarizations indicate that a point charge model is a poor approximation of the electronic distribution about the metal cation and its two

dx.doi.org/10.1021/ic300394c | Inorg. Chem. 2012, 51, 4862−4868

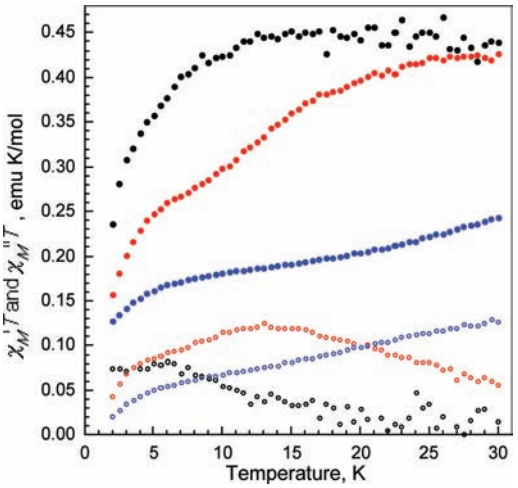

Figure 6. Temperature dependence of $\chi_M'T$, solid points, and $\chi_M''T$, open points, for $Cu(5\text{-}ATZ)_4Cl_2$, **2**, obtained upon warming from 2 to 30 K in a ±3 Oe ac field and a 1000 Oe dc bias field. The black points have been obtained at 311 Hz, the red points at 2311 Hz, and the blue points at 9011 Hz.

axial chloride ligands. Both **1** and **2** belong[1c] to the class of three-dimensional framework ferroelectrics and their remanent and saturation polarizations and coercive fields are within the broad range of values observed[1c,2] for many ferroelectric metal–organic complexes.

CONCLUSIONS

Two acentric mononuclear complexes, $Co(5\text{-}ATZ)_4Cl_2$, **1**, and $Cu(5\text{-}ATZ)_4Cl_2$, **2**, where 5-ATZ is the monodentate 5-amino-1-H-tetrazole ligand, have been synthesized and their structural, magnetic, and ferroelectric properties have been studied. Both complexes crystallize in the *P4nc* space group, a member of the polar noncentrosymmetric 4*mm* class, a class that may exhibit both ferroelectric and nonlinear optical properties. The tetrazole rings of the four 5-ATZ ligands in **1** and **2** are not coplanar but rather they are arranged like the blades of a propeller and, although an isolated molecule of **1** or **2** would be chiral, the symmetry operations associated with the *P4nc* space group make **1** and **2** achiral. In agreement with the properties of the polar noncentrosymmetric 4*mm* class, **1** and **2** show ferroelectric hysteresis loops at room temperature with saturation polarizations of 0.034 and 0.031 $\mu C/cm^2$, remanent polarizations of 0.015 $\mu C/cm^2$, and coercive electric fields of 5.5 and 5.7 kV/cm, respectively. This ferroelectric behavior is likely to result from the off-centering of the metal cation located between its two axial chloride neighbors. Hence, it would be interesting to follow the changes in the crystal structure as the temperature increases above the ferroelectric Curie temperature of these complexes, a temperature that has not been determined herein and may well be above the decomposition temperature of these complexes.

Magnetic studies indicate that **1** is a paramagnetic high-spin cobalt(II) complex with a rather extensive spin–orbit coupling, modeled as a zero-field splitting parameter, D, of $\pm 91(3)$ cm^{-1} and with very weak long-range antiferromagnetic exchange interactions. Direct current and ac magnetic studies indicate that **2** is a paramagnetic copper(II) complex that exhibits weak ferromagnetic exchange interactions below 15 K. Unfortunately, neither compound exhibits a ferromagnetic hysteresis loop above 2 K, and the search for a multiferroic metal organic complex is still open.

ASSOCIATED CONTENT

Supporting Information

Structure of **1**, cif files for **1** and **2**, and additional details of the analysis of the magnetic results. This material is available free of charge via the Internet at http://pubs.acs.org.

AUTHOR INFORMATION

Corresponding Author

*E-mail: jmzheng@nankai.edu.cn (J.-M.Z.); glong@mst.edu (G.J.L.).

Notes

The authors declare no competing financial interest.

ACKNOWLEDGMENTS

The authors would like to thank Prof. Pierre Panissod of the University of Strasbourg for many helpful discussions during the course of this work. This work was supported by the National Natural Science Foundation of China (No. 50872057) and the Specialized Research Fund for the Doctoral Program of Higher Education of China (No. 20090031110013).

REFERENCES

(1) (a) Ye, Q.; Wang, X. S.; Zhao, H.; Xiong, R. G. *Chem. Soc. Rev.* **2005**, *34*, 208. (b) Zhao, H.; Qu, Z. R.; Ye, H. Y.; Xiong, R. G. *Chem.*

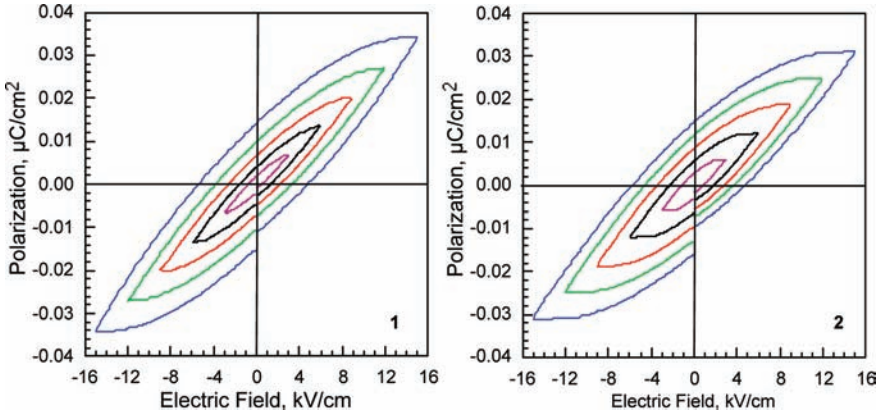

Figure 7. Electric hysteresis loops obtained at ambient temperature with pellets of powdered $Co(5\text{-}ATZ)_4Cl_2$, **1**, left, and $Cu(5\text{-}ATZ)_4Cl_2$, **2**, right, in applied fields of ±3, ±6, ±9, ±12, and ±15 kV/cm for the successive loops.

dx.doi.org/10.1021/ic300394c | *Inorg. Chem.* 2012, 51, 4862–4868

Soc. Rev. **2008**, *37*, 84. (c) Hang, T.; Zhang, W.; Ye, H. Y.; Xiong, R. G. *Chem. Soc. Rev.* **2011**, *40*, 3577. (d) Kong, F.; Huang, S. P.; Sun, Z. M.; Mao, J. G.; Cheng, W. D. *J. Am. Chem. Soc.* **2006**, *128*, 7750. (e) Jain, P.; Ramachandran, V.; Clark, R. J.; Zhou, H. D.; Toby, B. H.; Dalal, N. S.; Kroto, H. W.; Cheetham, A. K. *J. Am. Chem. Soc.* **2009**, *131*, 13625.

(2) Zhang, W.; Ye, H. Y.; Xiong, R. G. *Coord. Chem. Rev.* **2009**, *253*, 2980.

(3) Halasyamani, P. S.; Poeppelmeier, K. R. *Chem. Mater.* **1998**, *10*, 2753.

(4) The corresponding 10 point group symmetries are given in parentheses after the crystal classes: 1 (C_1), *m* (C_s), 2 (C_2), *mm*2 (C_{2v}), 3 (C_3), 3*m* (C_{3v}), 4 (C_4), 4*mm* (C_{4v}), 6 (C_6), and 6*mm* (C_{6v}).

(5) (a) Eerenstein, W.; Mathur, N. D.; Scott, J. F. *Nature* **2006**, *442*, 759. (b) Cui, H. B.; Wang, Z. M.; Takahashi, K.; Okano, Y.; Kobayashi, H.; Kobayashi, A. *J. Am. Chem. Soc.* **2006**, *128*, 15074. (c) Ohkoshi, S.; Tokoro, H.; Matsuda, T.; Takahashi, H.; Irie, H.; Hashimoto, K. *Angew. Chem., Int. Ed.* **2007**, *46*, 3238. (d) Rogez, G.; Viart, N.; Drillon, M. *Angew. Chem., Int. Ed.* **2010**, *49*, 1921.

(6) (a) Ye, Q.; Hang, T.; Fu, D. W.; Xu, G. H.; Xiong, R. G. *Cryst. Growth Des.* **2008**, *8*, 3501. (b) Hang, T.; Fu, D. W.; Ye, Q.; Xiong, R. G. *Cryst. Growth Des.* **2009**, *9*, 2026.

(7) Holman, K. T.; Pivovar, A. M.; Ward, M. D. *Science* **2001**, *294*, 1907.

(8) (a) Okubo, T.; Kawajiri, R.; Mitani, T.; Shimoda, T. *J. Am. Chem. Soc.* **2005**, *127*, 17598. (b) Song, L.; Du, S. W.; Lin, J. D.; Zhou, H.; Li, T. *Cryst. Growth Des.* **2007**, *7*, 2268. (c) Su, Z.; Chen, M. S.; Fan, J.; Chen, M.; Chen, S. S.; Luo, L.; Sun, W. Y. *CrystEngComm* **2010**, *12*, 2040.

(9) (a) He, X.; Lu, C. Z.; Yuan, D. Q. *Inorg. Chem.* **2006**, *45*, 5760. (b) Wang, X. W.; Chen, J. Z.; Liu, J. H. *Cryst. Growth Des.* **2007**, *7*, 1227. (c) Yao, Y. L.; Xue, L.; Che, Y. X.; Zheng, J. M. *Cryst. Growth Des.* **2009**, *9*, 606. (d) Liu, D. S.; Huang, X. H.; Huang, C. C.; Huang, G. S.; Chen, J. Z. *J. Solid State Chem.* **2009**, *182*, 1899.

(10) Bain, G. A.; Berry, J. F. *J. Chem. Educ.* **2008**, *85*, 532.

(11) *CrystalClear*, version 1.3.5; Rigaku Corp.: Woodlands, TX, 1999.

(12) Sheldrick, G. M. *SHELX-97, Suite of programs for solution and refinement of crystal structures*; University of Göttingen: Göttingen, Germany, 1997.

(13) Flack, H. D. *Acta Crystallogr.* **1983**, *A39*, 876.

(14) Crystal and refinement parameters for **1**: $CoC_4H_{12}N_{20}Cl_2$, molecular wt = 470.17 g/mol, tetragonal, *P*4*nc*, $a = b = 9.7393(14)$ Å, $c = 8.4141(17)$ Å, $\alpha = \beta = \gamma = 90°$, $V = 798.1(2)$ Å^3, $Z = 2$, $D_c = 1.956$ g/cm^3, $R_1 = 0.0204$, $wR_2 = 0.0588$, $\mu = 1.456$ mm^{-1}, $S = 1.001$, and Flack = 0.036(15). Crystal and refinement parameters for **2**: $CuC_4H_{12}N_{20}Cl_2$, molecular wt = 474.78 g/mol, tetragonal, *P*4*nc*, $a = b = 9.5134(10)$ Å, $c = 8.8507(19)$ Å, $\alpha = \beta = \gamma = 90°$, $V = 801.0(2)$ Å^3, $Z = 2$, $D_c = 1.968$ g/cm^3, $R_1 = 0.0213$, $wR_2 = 0.0533$, $\mu = 1.743$ mm^{-1}, $S = 1.000$, and Flack = 0.023(15).

(15) (a) Thomas, L.; Lionti, F.; Ballou, R.; Gatteschi, D.; Sessoli, R.; Barbara, B. *Nature* **1996**, *383*, 145. (b) Gatteschi, D.; Sessoli, R. *Angew. Chem., Int. Ed.* **2003**, *42*, 268. (c) Freedman, D. E.; Harman, W. H.; Harris, T. D.; Long, G. J.; Chang, C. J.; Long, J. R. *J. Am. Chem. Soc.* **2010**, *132*, 1224.

(16) (a) Lin, P. H.; Burchell, T. J.; Clérac, R.; Murugesu, M. *Angew. Chem., Int. Ed.* **2008**, *47*, 8848. (b) Rinehart, J. D.; Long, J. R. *J. Am. Chem. Soc.* **2009**, *131*, 12558. (c) Wang, Y.; Li, X.-L.; Wang, T.-W.; Song, Y.; You, X.-Z. *Inorg. Chem.* **2010**, *49*, 969. (d) Rinehart, J. D.; Meihaus, K. R.; Long, J. R. *J. Am. Chem. Soc.* **2010**, *132*, 7572.

(17) Kahn, O. *Molecular Magnetism*; VCH Publishers: New York, 1993; p 38.

(18) Murrie, M. *Chem. Soc. Rev.* **2010**, *39*, 1986.

(19) Lloret, F.; Julve, M.; Cano, J.; Ruiz-Garcia, R.; Pardo, E. *Inorg. Chim. Acta* **2008**, *361*, 3432.

(20) Carlin, R. L.; van Duyneveldt, A. J. *Magnetic Properties of Transition Metal Compounds*; Springer-Verlag: New York, 1977; p 119.

(21) Oja, T.; Casabella, P. A. *Phys. Rev.* **1969**, *177*, 830.